Floating Small Target Detection in Sea Clutter Based on Jointed Features in FRFT Domain

Yan-ling Shi(✉), Xue-liang Zhang, and Zi-peng Liu

College of Telecommunications and Information Engineering,
Nanjing University of Post and Telecommunications, Nanjing 210003, China
{ylshi,l2l7012431,l2l8012603}@njupt.edu.cn

Abstract. The jointed-feature detector for the floating small target in sea clutter is addressed in the paper. For the traditional energy-based detectors, it is difficult to detect the low signal-to-clutter ratio floating small target in time domain due to the affection of sea clutter motion. Therefore, a feature detector in the Fractional Fourier transform (FRFT) domain is proposed. The Hurst exponent and fractal dimension variance are extracted as the features in the jointed-feature detector in FRFT domain. The decision region is determined by convex hull training algorithm on the given false alarm probability. The experimental results of 10 groups of IPIX radar data show that the jointed-feature detector is superior to the compared one, and it provides a new detection scheme for radar target detection.

Keywords: Fractional Fourier Transform · Jointed features · Convex hull training algorithm · Target detection · Sea clutter

1 Introduction

The traditional energy accumulation detectors are statistically optimal in the case of linear, stationary and Gaussian sea clutter. However, the high range resolution sea clutter is nonlinear, non-stationary and non-Gaussian. Therefore, the accumulation detectors inevitably decline the detection performance for the high range resolution sea clutter [1, 2]. Hence, we resort to feature detectors [3–7] which get rid of the energy accumulation. The existing feature detectors mainly use the polarization features [3], normalized Doppler power spectrum features [4], related features [5], speckle consistency factor [6], ridge energy characteristics in the time-frequency plane, etc. [7]. The experimental results evidence the effectivity of those feature detectors.

In order to understand the scattering of sea surface deeply, fractal describes the roughness of the sea surface, and it is used to detect the floating target in sea clutter [8]. With the development of the fractal theory, it is found that a single fractal dimension failed to detect the floating target [9]. Therefore, the multi-dimensional fractal detectors were successively proposed [10–12]. The fractal and multi-dimensional fractal

This work was supported by National Natural Science Foundation of China (61201325) and NUPTSF (NY218045).

G. Gui and L. Yun (Eds.): ADHIP 2019, LNICST 302, pp. 128–139, 2019.
https://doi.org/10.1007/978-3-030-36405-2_14

detectors utilize the Hurst parameter [10], the geometric correlation coefficient of fractal [11, 12], and the multi-fractal features time domain feature [13] to distinguish between sea clutter and target. However, due to the energy overlap of sea clutter and floating target in the time domain, the time domain fractal features of clutter and target can not be distinguished, hence those fractal features are invalid. Many researchers captured the combining fractal theory in spectrum analysis [14–16], including Fourier transform combined with fractal [14], wavelet decomposition combined with fractal [15], Fractional Fourier Transform (FRFT) combined with fractal [16] and so on. FRFT as an extension of Fourier transform, selects an appropriate transformed order, and forms an obvious energy peak in the transform domain by all the energy accumulation. So, the fractal features in the FRFT domain can be used to distinguish target and sea clutter, and the jointed-feature detector in the FRFT domain is proposed in the paper. It has been verified that the sea clutter behaves the fractal characteristics in the FRFT domain, and the fractal-dimension detector in the FRFT domain achieves the good detection performance for the floating target in sea clutter [17].

As well known, the fractal features of the sea clutter will change with the sea state, wind speed and other uncertain factors. The pre-existing fractal detectors only utilizing a single feature in the time domain or frequency domain inevitable decline the detection performance in real scenario. Thus, by extracting the frequency domain kurtosis (FDK), Doppler entropy value and Doppler peak value, a jointed-feature detector was proposed [18], and improved the detection performance.

Combined the ideas of the feature detector in FRFT domain and of the jointed-detector, the jointed-feature detector in the FRFT domain is proposed in the paper. Firstly, the received radar echoes are converted to the FRFT domain; Secondly, the fractal features are analyzed by the Detrended Fluctuation Analysis (DFA), both the fractal dimension (FD) and fractal dimension variance (FDV) are extracted; Finally, the jointed-feature detector is proposed by using the two features. The decision region are determined based on the convex hull training algorithm for pure clutter in the FRFT domain, and the efficiency of the proposed detector is verified by the measured data.

The innovation is the FD and FDV as two features in the FRFT domain helping to get rid of the energy overlap of floating target and sea clutter in the time domain.

This paper is organized as follows: Sect. 2 analyzes the fractal characteristics of sea clutter and targets in the FRFT domain, and extracts two fractal features in the optimal FRFT domain, that is FD and FDV; Sect. 3 proposes the jointed-feature detector, and gives the flow chart. In Sect. 4, the efficiency of the proposed detector is verified by the measured data. Finally, conclude the whole paper in Sect. 5.

2 Characteristic Analysis of Sea Clutter in FRFT Domain

The experiment data are collected by the IPIX radar [19] at dwelling mode, and contain 10 sea clutter datasets. Each dataset consists of 14 adjacent range cells with 131 072 sampling points (about 131 s). Target is a styrofoam ball wrapped with wire mesh with a diameter about 1 m. The range cell where the target is located is called primary cell, and two or three cells neighbor of the primary cell are affected by the target and are called guard cells. Other range cells are called secondary cells. The range resolutions of

these 10 datasets are 30 m. Table 1 lists the relevant parameters of 10 datasets, including their file names in the IPIX datasets, wind speed (WS), significant wave height, the angle between the line of radar sight and wind direction, and the numbers of the primary cells and secondary cells.

Table 1. Description of IPIX radar datasets

Label	File name	Wind speed (Km/h)	Wave height (M)	Angle	Primary	Secondary
1	19931107_135603_starea17	9	2.2	9	9	8,10,11
2	19931108_220902_starea26	9	1.1	97	7	6,8
3	19931109_191449_starea30	19	0.9	98	7	6,8
4	19931109_202217_starea31	19	0.9	98	7	6,8,9
5	19931110_001635_starea40	9	1.0	88	7	5,6,8
6	19931111_163625_starea54	20	0.7	8	8	7,9,10
7	19931118_023604_stareC0000280	10	1.6	130	8	7,9,10
8	19931118_162155_stareC0000310	33	0.9	30	7	6,8,9
9	19931118_162658_stareC0000311	33	0.9	40	7	6,8,9
10	19931118_174259_stareC0000320	28	0.9	30	7	6,8,9

2.1 Statistical Analysis of Sea Clutter in FRFT Domain

As an extension of the Fourier transform, the FRFT is also called generalized time-frequency analysis. The p-order FRFT of $x(t)$ is a linear integral operation [20] as

$$\mathrm{F}_p(u) = \int_{-\infty}^{+\infty} x(t) K_p(t,u) dt \tag{1}$$

where the kernel function $k_p(t,u)$ is,

$$K_p(t,u) = \begin{cases} \sqrt{\frac{1-j\cos\alpha}{2p}} \exp(j\frac{t^2+u^2}{2}) \cot\alpha - jut\csc\alpha, & \alpha \neq n\pi \\ \delta(t-u), & \alpha \neq 2n\pi \\ \delta(t+u), & \alpha = (2n+1)\pi \end{cases} \tag{2}$$

where, $\alpha = \frac{p\pi}{2}$ is the rotation angle and p is the transformed order in the FRFT.

Figure 1 shows the amplitudes of target and clutter in the time domain and FRFT domain, respectively. The experimental data is 19931107_ 135603_starea17 in HH polarized, and the optimal transformed-order of FRFT is taken as p = 1.056. From Fig. 1, in the time domain, the amplitudes of target and sea clutter are overlapped with each other, which is bad for the target detection. In the FRFT domain, the target energy behaves an obvious peak, several orders larger than the clutter energy, which is beneficial for target detection.

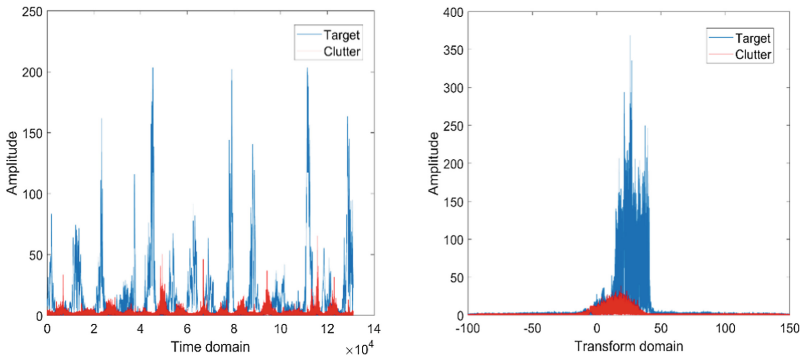

Fig. 1. Amplitudes target and sea clutter in the time domain and in the FRFT domain.

2.2 Fractal Features Extraction

Sea clutter behaves the fractional Brownian motion (FBM), and the Hurst exponent can capture all the properties of FBM, as confirmed in [14]. For the IPIX measured radar data, the DFA describes the fractal features of the received echoes. Assuming that $x(n), 0 < n \leq N$ is a N stationary random sequence, the DFA of $x(n)$ includes the following six steps [17],

Step 1, calculate the cumulative difference of $x(n)$, and obtain a new sequence $y(n)$,

$$y(n) = \sum_{i=1}^{n} [x(i) - \overline{x}], n > 0 \tag{3}$$

where, $\bar{x}$ is the average of the time series $x(n)$.

Step 2, suppose the length of the segment is m. Divide the new sequence $\mathrm{y}(n)$ into disjoint sequences $y[(s-1)m+n]$ with equal length m, where $s = 1, 2, 3 \cdots N_m$, $N_m = INT(N/m)$, N_m is the number of segments, and INT is the rounding operation.

Step 3, if the time series length N is not an integral multiple of m, the segment sequences of $\mathrm{y}(n)$ are taking from the end of the sequence $y[N-(s-N_m)m+n]$, where, $s = N_m + 1, N_m + 2, \cdots, 2N_m$. Combined with steps 2 and 3, a total of $2N_m$ sequences are formed.

Step 4, linear fit each subsequence by using the least squares fitting and calculate the local trend term of the subsequence $\mathrm{y}_s(n)$

$$y_s(n) = fit(y(n)) = ax + b \tag{4}$$

where, a and b are the fitting coefficients.

Step 5, each subsequence subtracts its local trend term $\mathrm{y}_s(n)$, and find its variance

$$Y^2(s,m) = \frac{1}{m}\sum_{n=1}^{m} \{y[(s-1)m+n] - y_s(n)\}^2 \quad s = 1, 2, 3 \cdots N_m \tag{5}$$

$$Y^2(s,m) = \frac{1}{m}\sum_{n=1}^{m}\{y[N-(s-N_m)m+n] - y_s(n)\}^2 \quad s = N_m+1, N_m+2, \cdots, 2N_m \tag{6}$$

Step 6, average the variance of each subsequence, and calculate the q-th root, we obtain the q-order wave function

$$F_q(m) = \left\{\frac{1}{2N_m}\sum_{s=1}^{2N_m}[Y^2(s,m)]\right\}^{1/q} \tag{7}$$

If the time series is long correlated, $F(m)$ will grow with m

$$F(m) \sim m^H \tag{8}$$

where, H is the Hurst exponent, reflecting the fractal parameters of $F(m)$.

The wave function of received echo in scale-invariant space is

$$\log_2 F(m) = (2 - F_d)\log_2(m) + I_c \tag{9}$$

where the fractal dimension F_d can be obtained by linear fitting, $F_d = 2 - H$.

Fractal dimension can approximately reflect the irregularity of data [21]. The fractal features of the target and clutter are different to some extent. Therefore, we can distinguish sea clutter and target by F_d in FRFT domain. The first test statistic is as follows,

$$T_1 = |F_d| \underset{\mathrm{H_1}}{\overset{\mathrm{H_0}}{\gtrless}} \eta_1 \tag{10}$$

where, T_1 is the test statistic and η_1 is the detection threshold.

The ideal fractal curve satisfies the self-similarity of all scales, which means that F_d is independent of the scale m. It is found that the fractal features of sea clutter in the FRFT domain are in good agreement with the theoretical fractal model in the scale-invariant space [20]. The double logarithmic coordinates of the fractal curve in the FRFT domain can be expressed as x_i and y_i

$$\begin{cases} x_i = \log_2(m_i) \\ y_i = \log_2 F(m_i) \end{cases} \tag{11}$$

where, m_i is the segment length of the i-th segment.

The fractal dimension $F_{\Delta i}$ in the adjacent scale i is expressed as:

$$F_{\Delta i} = \frac{\log_2 F(m_i) - \log_2 F(m_{i-1})}{\log_2(m_i) - \log_2(m_{i-1})} = \frac{y_i - y_{i-1}}{x_i - x_{i-1}} \tag{12}$$

It has been verified in measured data that for different scales, $F_{\Delta i}$ changes weakly in secondary data, whereas significantly in primary data [22]. The fractal dimension variance V_d in the FRFT domain is used as a feature for target detection,

$$V_d = \mathrm{var}(F_{\Delta i}) \tag{13}$$

The second test statistic is as follows,

$$T_2 = V_d \underset{\mathrm{H_0}}{\overset{\mathrm{H_1}}{\gtrless}} \eta_2 \tag{14}$$

where, η_2 is the detection threshold.

3 Jointed-Feature Detector in FRFT Domain

We propose a jointed-feature detector in FRFT domain by using F_d and V_d as two features to detect the floating target in the background of high range resolution sea clutter. The linear invariant interval is determined according to the fractal curve in FRFT domain. At the given false alarm rate, the convex hull training algorithm is used to determine the decision region, which can determine the classified samples and the training samples, and target can be detected according to whether inside or outside of the convex hull. The flow chart is shown in Fig. 2.

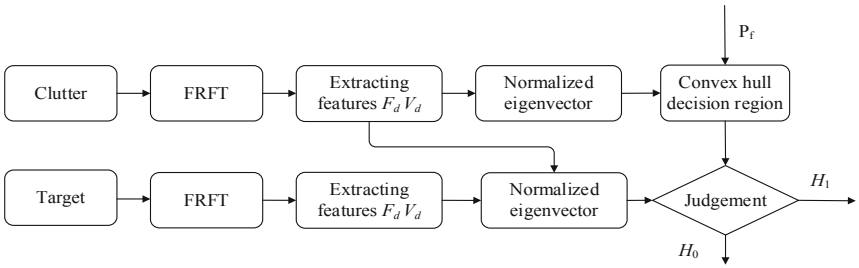

Fig. 2. The flow chart of jointed-feature detector in FRFT domain.

Set $y = [T_1, T_2]^T$, where the superscript T indicates transposition, and define $y_k = [T_1, T_2]_k^T$, $k = 1, 2, 3 \cdots K$, for the features of clutter. In order to obtain the smallest convex hull, given the false alarm rate P_f, $G = KP_f$ samples farthest from the center of the cluster are removed, and the remain $(K - G)$ samples are used to form convex hull as the discriminating area Ω [23].

For $(K - G)$ samples in a two-dimensional plane, a convex hull is a convex polygon consisting of the smallest convex set of $(K - G)$ samples. Let v_i, $i = 1, 2 \cdots I$ be the I vertices clockwise of the convex hull. For the sample y to be classified, the detecting principle is equivalent to judge whether y is inside or outside Ω. If and only if Eq. (15) holds [24],

$$r_i(y) \triangleq \begin{vmatrix} 1 & v_i(1) & v_i(2) \\ 1 & v_{i+1}(2) & v_{i+1}(2) \\ 1 & y(1) & y(2) \end{vmatrix} \geq 0,\ i = 1, 2, \cdots, I \tag{15}$$

We can say if y is inside Ω, for all i, $r_i(y) \geq 0$. If y is outside Ω, $r_i(y) \geq 0$ for some i and $r_i(y) < 0$ for other i. Therefore, as long as $r_i(y) < 0$, we can determine that y is outside Ω. Based on the above analysis, the discriminant function is defined as

$$r(y) = \min\{r_i(y), i = 1, 2, \cdots, I\} \tag{16}$$

$r \geq 0$ means that $x(n)$ dose not contain target, and $r < 0$ indicates that $x(n)$ contains target.

Figure 3(a) shows the 24000 training samples and 4000 samples to be classified in the 2D feature plane, and Fig. 3(b) shows both 4000 samples to be classified and the convex hull of (24000-240) training samples by removing the 240 farthest training samples. The blue points are the training samples and red points are the samples to be classified. From Fig. 3, the convex hull training algorithm can effectively distinguish the samples to be classified from the training samples.

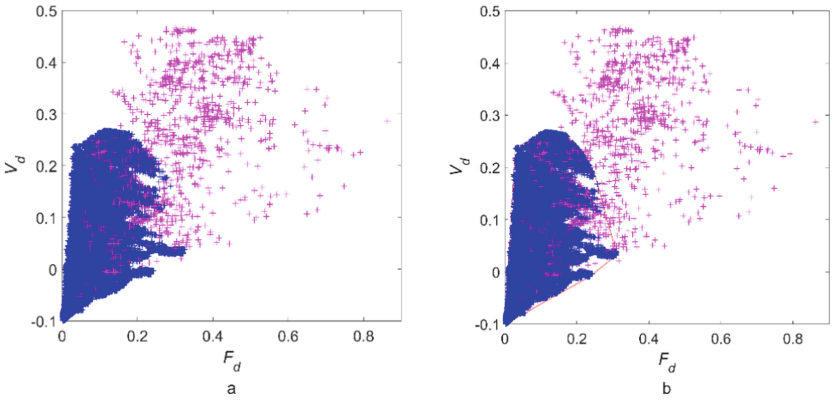

Fig. 3. The samples to be classified (red) and the training samples (blue) in the two-dimensional feature plane. (Color figure online)

4 Experimental Results

4.1 Analysis of Fractal Features in Measured Data

Sea clutter behaves obvious fractal Brownian motion, but has self-similarity only in the scale-free interval [14]. Figure 4 is a log-log $F(m) \sim m$ in FRFT domain of 10 datasets in HH polarization. The circled red lines represent the log-log functions of the target, and the asterisk blue lines represent the log-log wave functions of clutter. The experimental parameters are $n = 10000$, $m = 2^1 \sim 2^{10}$. From Fig. 4, for the 10

datasets, when m is $2^5 \sim 2^{10}$, the curves are approximately linear. Therefore, the interval $2^5 \sim 2^{10}$ can be taken as a scale-free interval for sea clutter. In the scale-free interval $2^5 \sim 2^{10}$, the slopes of the circled curves are larger than these of the star curves, indicating that the Hurst exponent of target is larger than that of clutter, in other words, target has a smaller fractal dimension than clutter.

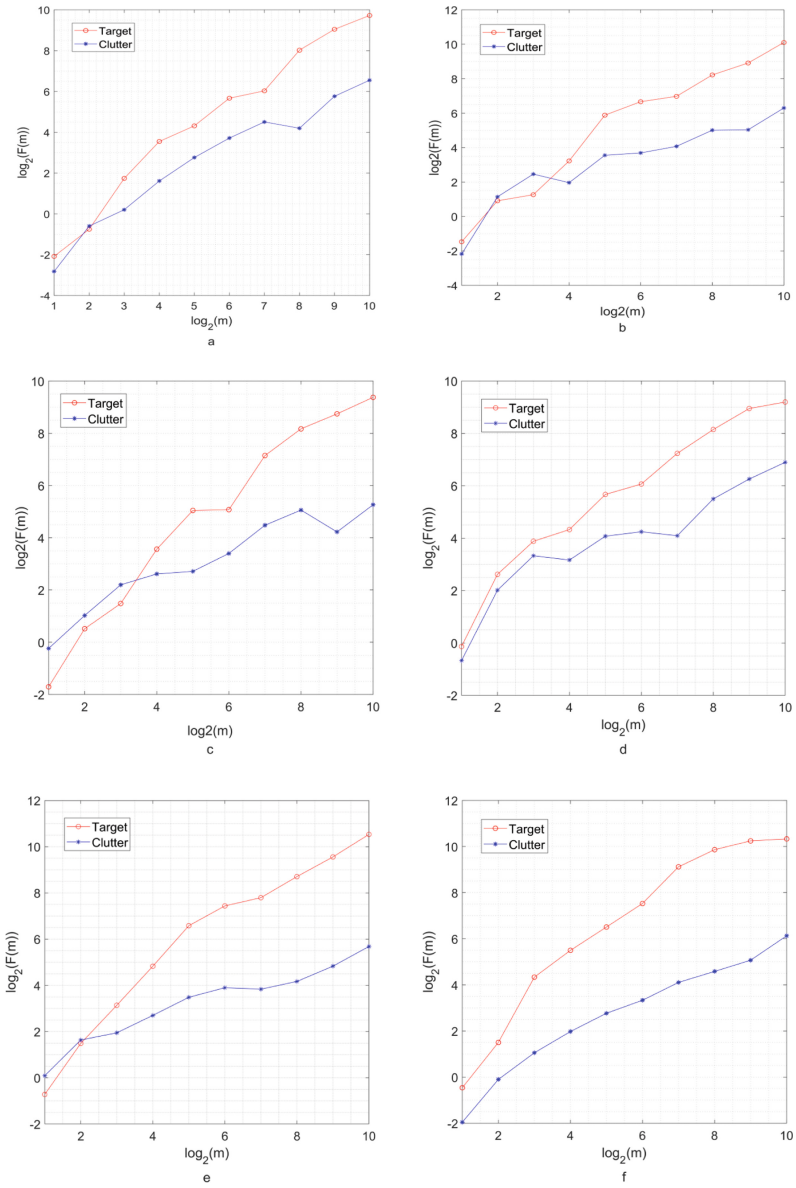

Fig. 4. (a-j). log-log wave functions in the FRFT domain of 10 datasets.

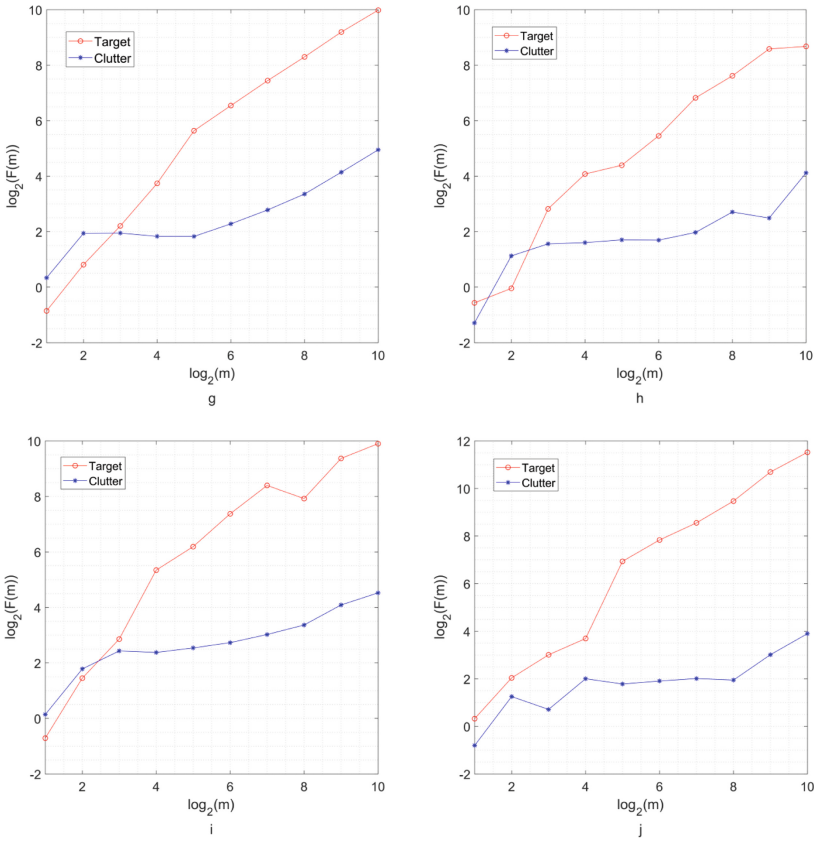

Fig. 4. (*continued*)

4.2 Performance Analysis of the Jointed-Feature Detector

In order to quantitatively compare the detection performance of the two single feature detectors with the jointed-feature detector, we use 19931107_135603_starea17. The experimental parameters are $n = 10000$ and $m = 2^5 \sim 2^{10}$. To satisfy the required samples in Monte Carlo test for a given small probability of false alarm, we slide 5 points for each adjacent segment to obtain 24000 datasets. Calculate F_d and V_d of each dataset in the scale-free space $[2^5 \sim 2^{10}]$. Figure 5 is the detection probabilities of F_d, V_d and the proposed jointed-feature detector, respectively. From Fig. 5, when false alarm probability equals 0.001, the detection probability of jointed-feature detector, F_d and V_d are $P_d = 0.918$, $P_d = 0.452$, and $P_d = 0.662$, respectively. It can be seen that the detection performance of the jointed-feature detector is significantly improved compared to the single feature detectors. The reason is that the jointed-feature detector utilizes the two-dimensional information of fractal, which increases the difference between the sea clutter and the target, and hence has a significant improvement in detection performance.

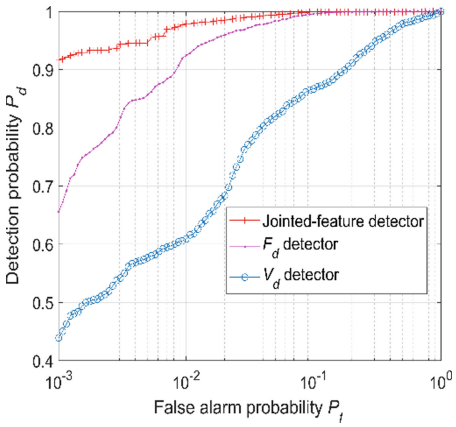

Fig. 5. Detection probabilities of the three detectors in 19931107_135603_starea17.

Table 2. Detection performance of three detectors, where false alarm rate is 0.001

Label	File name	F_d	V_d	Jointed-feature detector
1	19931107_135603_starea17	45.2%	66.2%	**91.8%**
2	19931108_220902_starea26	39.5%	55.7%	**89.2%**
3	19931109_191449_starea30	40.5%	55.9%	**90.5%**
4	19931109_202217_starea31	38.0%	50.8%	**87.6%**
5	19931110_001635_starea40	32.1%	47.5%	**86.4%**
6	19931111_163625_starea54	33.5%	46.5%	**83.7%**
7	19931118_023604_stareC0000280	42.4%	60.3%	**88.6%**
8	19931118_162155_stareC0000310	41.5%	63.2%	**81.3%**
9	19931118_162658_stareC0000311	36.8%	60.4%	**78.6%**
10	19931118_174259_stareC0000320	39.8%	55.7%	**78.5%**

Table 2 shows the detection probabilities of F_d, V_d and the proposed jointed-feature detector of all 10 datasets. When the false alarm probability equals 0.001, the detection probabilities in the jointed-feature detector of all 10 datasets are greatly higher than the single feature F_d and V_d. Therefore, the proposed jointed-feature detector is feasible in detecting small floating target on the sea surface.

5 Conclusion

In this paper, the fractal features of the received radar echo in FRFT domain are analyzed. By extracting the fractal dimension and FDV in the FRFT domain, the jointed-feature detector are proposed. The discriminating area of training samples is determined by the convex hull training algorithm. The experimental results show that the sea clutter satisfies the self-similarity in the scale-free interval m $\in [2^5, 2^{10}]$ in the

FRFT domain. The jointed-feature detector has a significant improvement in detection performance compared to the fractal dimension detector and the FDV detector by the 10 measured datasets. Therefore, the proposed jointed-feature detector is feasible in detecting small floating target on the sea surface.

References

1. You, H., Yong, H., Jian, G.: An overview on radar target detection in sea clutter. Mod. Radar **36**(12), 1–9 (2014)
2. Ding, H., Dong, Y., Liu, N.: Overview and prospects of research on sea clutter property cognition. J. Radars **5**(5), 499–516 (2016)
3. Xu, S., Zheng, J., Pu, J.: Sea-surface "floating small target detection based on polarization features". IEEE Geosci. Remote Sens. Lett. **15**(10), 1505–1509 (2018)
4. Li, D., Shui, P.: Floating small target detection in sea clutter via normalised Doppler power spectrum. IET Radar Sonar Navig. **10**(4), 699–706 (2016)
5. Ye, Y., Hong, Z., Wang, Q.: Correlation feature-based detector for range distributed target in sea clutter. EURASIP J. Adv. Signal Process. **2018**(1), 25 (2018)
6. Shi, Y., Xie, X., Li, D.: Distributed floating target detection in sea clutter via feature-based detector. IEEE Geosci. Remote Sens. Lett. **13**(12), 1847–1850 (2016)
7. Shi, S., Shui, P.: Sea-surface floating small target detection by one-class classifier in time-frequency feature space. IEEE Trans. Geosci. Remote Sens. **56**(11), 6395–6411 (2018)
8. Lo, T., Leung, H., Litva, J.: Fractal characterisation of sea-scattered signals and detection of sea-surface targets. In: IEEE Proceedings F Radar and Signal Processing, vol. 140, no. 4, pp. 243–250 (1993)
9. Li, D., Shui, P.: Extended fractal analysis for floating target detection in sea clutter. In: IEEE International Geoscience and Remote Sensing Symposium, pp. 3139–3142 (2015)
10. Chen, Y., Sun, R., Zhou, A.: An improved Hurst parameter estimator based on fractional Fourier transform. In: Proceedings of the ASME 2007 International Design Engineering Technical Conferences & Computers and Information in Engineering Conference, Las Vegas, Nevada, USA, pp. 1–11 (2007)
11. Guan, J., Liu, N., Zhang, J.: Multifractal correlation characteristic of real sea clutter and low-observable targets detection. J. Electron. Inf. Technol. **32**(1), 54–61 (2010)
12. Hu, J., Gao, J., Yao, K.: Detection of low-observable targets within sea clutter by structure function based multifractal analysis. IEEE Trans. Antennas Propag. **54**(1), 136–143 (2006)
13. Guan, J., Liu, N., Huang, Y.: Fractal characteristic in frequency domain for target detection within sea clutter. IET Radar Sonar Navig. **6**(5), 293–306 (2012)
14. Chen, X., Guan, J., Bao, Z.: Detection and extraction of target with micromotion in spiky sea clutter via short-time Fractional Fourier Transform. IEEE Trans. Geosci. Remote Sens. **52**(2), 1002–1018 (2014)
15. Guan, J., Liu, N., Zhang, J.: Low-observable target detection within sea clutter based on LGF. Signal Process. **26**(1), 69–73 (2010)
16. Chen, X., Guan, J., He, Y.: Detection of low observable moving target in sea clutter via fractal characteristics in Fractional Fourier Transform domain. IET Radar Sonar Navig. **7**(6), 635–651 (2013)
17. Xing, H., Zhang, Q., Xu, W.: Fractal property of sea clutter FRFT spectrum for small target detection. Acta Phys. Sin. **1**, 1–8 (2015)
18. Shui, P., Li, D., Xu, S.: Tri-feature-based detection of floating small targets in sea clutter. IEEE Trans. Aerosp. Electron. Syst. **50**(2), 1416–1430 (2014)

19. Haykin, S.: The McMaster IPIX radar sea clutter database in 1993. http://soma.mcmaster.ca/ipix.php
20. Li, Y., Lv, X., Liu, K.: Fractal-based weak target detection within sea clutter. Acta Ocean. Sin. **33**(9), 68–72 (2014)
21. Xu, X.: Low observable targets detection by joint fractal properties of sea clutter: an experimental study of IPIX OHGR datasets. IEEE Trans. Antennas Propag. **58**(4), 1425–1429 (2010)
22. Guan, J., Cheng, X., Huang, Y.: Adaptive Fractional Fourier Transform-based detection algorithm for moving target in heavy sea clutter. IET Radar Sonar Navig. **6**(5), 389–401 (2012)
23. Xing, H., Yin, J., Wang, Q.: Targets detection under the background of sea clutter by joint characteristics difference. Mod. Radar **36**(10), 28–32 (2014)
24. Shi, Y., Shui, P.: Feature united detection algorithm on floating small target of sea surface. J. Electron. Inf. Technol. **34**(4), 871–877 (2012)